

EFFECT OF THE LOCATION AND WIDTH OF CFRP BANDS ON ECCENTRICALLY COMPRESSED CFRP BAND-CONFINED SSRC COLUMNS

ẢNH HƯỞNG CỦA VỊ TRÍ VÀ BỀ RỘNG CỦA BẢN CFRP ĐẾN CỘT BÊ TÔNG CỐT THÉP TIẾT DIỆN VUÔNG ĐƯỢC GIA CƯỜNG BỞI BẢN CFRP DƯỚI TÁC DỤNG CỦA TẢI TRỌNG LỆCH TÂM

Anh Duc Mai^{1*}, Ngoc Duong Vo¹, Van Huong Nguyen¹, Phuoc Dung Tran², Van Tuoi Nguyen²

¹The University of Danang - University of Science and Technology, Danang, Vietnam

²Central College of Transport V, Danang, Vietnam

*Corresponding author: maduc@dut.udn.vn

(Received: January 19, 2024; Revised: February 27, 2024; Accepted: February 28, 2024)

Abstract - The effectiveness of FRP in retrofitting/strengthening existing steel reinforced concrete (SRC) structures has been widely recognized. However, investigation on the performance of CFRP band-confined square SRC (CFRPBC-SSRC) columns are still limited. This paper compares the performance of SSRC columns without and with different CFRP bands to examine the effect of the location and width of CFRP bands on the performance of CFRPBC-SSRC. The test results exhibited that SSRC columns obtained a considerable enhancement in the ductility and load-bearing capacity (LBC) by strengthening with CFRP bands. At the same amount of CFRP employed, SSRC columns confined discontinuously with CFRP bands placed in between lateral ties under concentric and eccentric compression obtained higher LBC and ductility than their counterparts confined discontinuously with CFRP bands without taking into account the location of lateral ties. The axial-flexural interaction diagrams of CFRPBC-SRC columns were established based on two codes of FIB-Bulletin-14 and ACI-440.2R-17.

Key words - Square columns; discontinuous confinement; FRP confined concrete; eccentric compression; strength diagram

1. Introduction

Strengthening/retrofitting of existing concrete structures may be required due to the load demand increase, the structure deterioration resulting from environment attack and excessive load and the correction of improper design and construction [1-3]. Strengthening or upgrading concrete structural members with FRPs has been widely applied and well recognized as an efficient solution as this solution takes full advantages of FR comprising corrosion free, high tensile strength and light weight [1, 2, 4-6] as well as ease to construct on site [7, 8].

Strengthening/retrofitting concrete columns with FRP is usually carried out by externally bonding FRP sheets on concrete columns in which the FRP fibres are arranged in transverse direction. The FRP jacket generates confining pressure when concrete expands, which in turn prevents concrete dilation, resulting in a remarkable enhancement in the column LBC and deformability [9-13]. Extensive investigation on the performance of FRP confined-SSRC columns (FRPC-SSRC columns) has been devoted during the last few decades; however, most of the available investigation focused on the performance of FRPC-SSRC columns under concentric compressions [1, 9, 14-20] and

Tóm tắt - Hiệu quả của vật liệu vải sợi FRP trong gia cường kết cấu bê tông cốt thép (SRC) đã được thừa nhận rộng rãi. Tuy nhiên, các nghiên cứu về sự làm việc của cột SRC tiết diện vuông (SSRC) gia cường gián đoạn bởi bản CFRP còn rất hạn chế. Nghiên cứu này so sánh sự làm việc của cột SSRC không gia cường và có gia cường không liên tục bởi các dải bản CFRP có bề rộng khác nhau nhằm đánh giá sự ảnh hưởng của bề rộng bản CFRP đối với ứng xử của cột SSRC. Kết quả nghiên cứu cho thấy rằng, các bản CFRP làm gia tăng đáng kể khả năng chịu tải và gia tăng lớn độ ổn định của cột SSRC. Cột SSRC được gia cường bởi bản CFRP đặt giữa cốt thép đai có khả năng chịu tải và có độ ổn định lớn hơn cột SSRC gia cường bởi bản CFRP không đặt giữa cốt thép đai. Nghiên cứu cũng xây dựng đường cong phá hoại của cột SSRC gia cường bởi bản CFRP dựa trên 02 tiêu chuẩn quốc tế là FIB-Bulletin-14 và ACI-440.2R-17.

Từ khóa - Cột tiết diện vuông; gia cường không liên tục; gia cường cột bê tông cốt thép bằng vải sợi FRP; cột chịu nén lệch tâm; đường cong phá hoại của cột bê tông cốt thép

fewer investigation considered the performance of FRPC-SSRC columns under eccentric compressions [3, 21-26]. In practice, a column is usually subject to eccentric axial compression because of its position (i.e., corner column) or accidental applied load resulting from construction errors [27]. It is well established that a higher magnitude of load eccentricity, a lower level of FRP confinement effectiveness [10, 21-23, 28-34].

In addition to the load eccentricity, the column cross-sectional shape substantially affects the FRP confinement efficiency. As the confining pressure generated by FRP jacket is non-uniformly distributed over square cross-sectional shape, the FRP confinement efficiency over square cross-section is much smaller than that over circular cross-section, which receives uniform FRP confining pressure [1, 3, 19, 35-38]. It is noted that the practical SRC columns are commonly formed in the square cross-section because of the low construction costs and the fast and easy construction of SSRC columns [39, 40]. Few investigation devoted to the performance of eccentrically-compressed FRPC-SSRC columns [8, 23-25, 30, 41-45].

Discontinuous FRP strengthening has been proven as an efficient strengthening solution along with continuous

FRP strengthening to improve the deformability and LCC of SSRC columns [8, 25, 30, 40, 46-52]. Discontinuous FRP strengthening has attracted a number of studies because of its practical advantages compared to continuous FRP strengthening, consisting of the possibility in eliminating air-bubble forming under the FRP jacket [53], less adhesive and FRP used [51] and the ease of construction [40, 53]. However, available investigation on the performance of eccentrically compressed CFRPBC-SSRC columns is inadequate [8, 25, 30, 45]. This investigation did not take into account the position of lateral ties in strengthening SSRC column with FRP bands. It is noted that the lateral confinement generated by discontinuous FRP confinement play an important role in preventing the concrete dilation, delaying cover concrete detachment and postponing longitudinal reinforcement buckling [30, 51, 54]. The longitudinal reinforcement buckling, which usually causes the FRP premature failure, is much more obvious for SSRC columns with sparse and insufficient transverse reinforcement [20, 51, 55, 56]. Therefore, it is expected that discontinuous strengthening of SSRC columns with CFRP bands placed in between the existing lateral ties may result in a better performance of CFRPBC-SSRC columns. Triantafyllou, et al. [51] experimentally found that, although the effective FRP confinement ratio (f_l/f_c) lower than minimum value of 0.07 for achieving a post-peak stress-strain response, the post-peak stress-strain response of CFRPBC-SSRC columns with bands located in between lateral ties under axial compression still showed ascending curves. Therefore, for deep understanding the effect of lateral ties' position on the flexural performance of CFRPBC-SSRC columns, the performance of CFRPBC-SSRC columns should be extensively studies.

The aforementioned literatures exhibits that the investigation on the effect of lateral ties on the performance of EC-CFRPBC-SSRC columns is not available yet in the literature. Additionally, the investigation on performance of eccentrically compressed CFRPBC-SSRC columns has been inadequate. Thus, this investigation examines the effect of the position and width of CFRP bands on the performance of EC-CFRPBC-SSRC columns. The main parameters are considered in this investigation consisting of different discontinuous strengthening schemes (non-strengthening, discontinuous strengthening without considering the position of lateral ties and discontinuous strengthening with CFRP bands placed in between lateral ties) and applied load eccentricity magnitudes.

2. Experimental Program

2.1. Specimen configuration

The test program consisted of twelve SSRC columns, which were cast from the one concrete batch and had an identical cross-sectional shape, length and reinforcement. Twelve SSRC columns having an identical height and side dimension, which were 800 mm and 150 mm; respectively. The longitudinal and transverse reinforcement of SSRC columns were, respectively, deformed and plain steel bars, which were 12-mm and 6-mm in diameter, respectively.

The height and side dimension of the SSRC columns were selected in line with ACI 318-11 [57] for capturing the performance of short columns. The spacing of lateral ties (b_s) is 80-mm. The 20 mm rounded corners (r_c) were implemented on the corners of SSRC columns as recommended in FIB Bulletin 14 [54] to improve the CFRP confinement efficiency for the CFRPBC-SSRC columns and to hinder the premature of CFRP strengthening at the two bottoms of the control SSRC columns. As the cover concrete of the SSRC columns at two ends and along the height was remained with a thickness of 20 mm, 760 mm deformed steel bars were employed to construct the SSRC columns. The details of the reinforcement and the geometry of the SSRC columns are graphically presented in Figure 1.

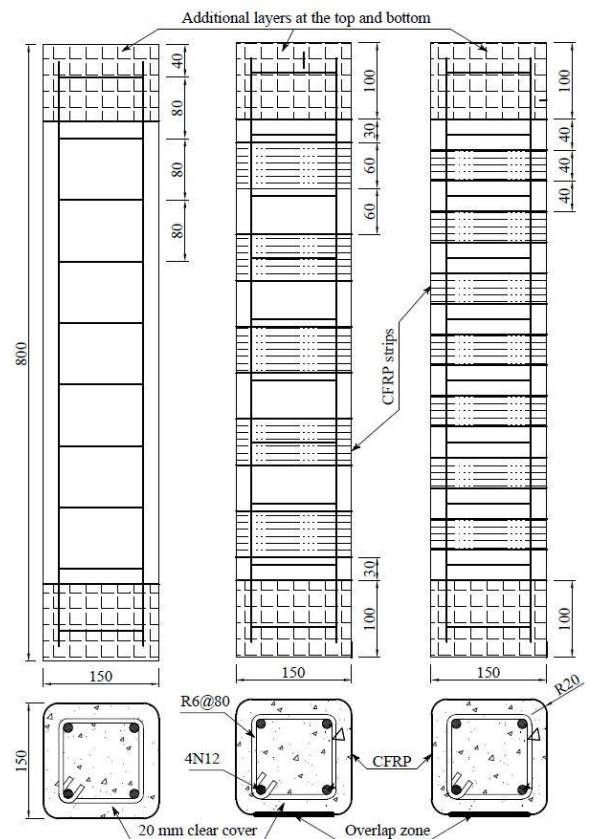


Figure 1. Details of the reinforcement and geometry of SSRC columns (mm): (1) Group SSRC-B0; (2) Group SSRC-B40; (3) Group SSRC-B60

The test program was designed to examine the effect of CFRP band width and its position on the performance of CFRPBC-SSRC columns, thus three groups of four columns (Groups of SSRC-B0, SSRC-B40 and SSRC-B60) with three CFRP strengthening systems were subjected to four different loads, which were concentric and eccentric compression (15 mm and 25 mm eccentricity) and pure bending. Group SSRC-B0 is the first group without external confinement, which was referred as the control group. Groups SSRC-B40 and SSRC-B60 (second and third groups, respectively) were discontinuously confined with 40 mm and 60 mm CFRP bands, respectively. For Groups SSRC-B40 and SSRC-B60, the clear distance of two consecutive bands (s_f) was taken to be the same the CFRP

band width (b_f) as commonly employed in some studies on discontinuous FRP strengthening available in the literatures [25, 30, 34, 47]. Accordingly, the b_f of Groups SSRC-B40 and SSRC-B60 was 40 mm and 60 mm, respectively. As Group SSRC-B40 considered the dual confinement of CFRP bands and lateral ties, thus the CFRP bands of Group SSRC-B40 were placed in between the lateral ties. Accordingly, the b_f of Group SSRC-B40 was a half of lateral ties' spacing. Also, one CFRP band of Group SSRC-B40 was placed at the column height. In contrast, Group SSRC-B60 did not take into consideration the dual confinement of CFRP bands and lateral ties, thus one CFRP band of Group SSRC-B60 was placed at the column mid-height while remaining bands placed along the height with the clear distance of two consecutive bands was 60 mm. Due to the difference of the CFRP band width, the total amount of CFRP employed for each column of Group SSRC-B60 (898,500 mm²) was slightly higher than that of each column of Group SSRC-B40 (862,560 mm²). The total amount of CFRP employed for each column was computed as the product of the CFRP plies, width and length. It should be mentioned here that

these three groups were separately presented in previous studies of the first author. In fact, Groups of SSRC-B0, and SSRC-B60 can be found in [58] while Group SSRC-B60 can be found in Mai, et al. [59]. It is also important to clarify that, Groups of SSRC-B0, SSRC-B40 and SSRC-B60 were assembled in this study to examine the effect of CFRP band width and its position on the performance of CFRPBC-SSRC columns, which were not taken into consideration in the previous studies.

The columns of Groups SSRC-B40 and SSRC-B60 were externally confined with CFRP bands using wet lay-up process in which each ply of the CFRP bands were saturated in the adhesive, which was made by mixing the hardener into adhesive resin with the ratio of 1:5. The outer ply of CFRP band was ended when the overlapping length of CFRP band was 100 mm, which was utilized to provide sufficient bond for CFRP bands. The CFRP bands having a width of 100 mm were also employed to externally confine the column two ends to inhibit the column premature failure resulted from the stress concentration. The detailed configuration of each group is presented in Table 1.

Table 1. Configuration of SSRC columns

Column	Longitudinal and transverse reinforcement	Type of wrapping	w_f (mm)	s_f (mm)	A (mm ²)	e (mm)
SSRC-B0-E0						0
SSRC-B0-E15	4N12 and R6@80	None	-	-	-	15
SSRC-B0-E25						25
SSRC-B0-B						Bending
SSRC-B60-E0						0
SSRC-B60-E15	4N12 and R6@80	Discontinuous strengthening without considering lateral ties	60	60	898,500	15
SSRC-B60-E25						25
SSRC-B60-B						Bending
SSRC-B40-E0						0
SSRC-B40-E15	4N12 and R6@80	Discontinuous strengthening in between lateral ties	40	40	862,560	15
SSRC-B40-E25						25
SSRC-B40-B						Bending

$$A = \text{Amount of CFRP used per specimen} = (\text{length}) \times (\text{width}) \times (\text{number of plies})$$

As presented in Table 1, the column of each group was given a label which consists of three portions separated by a dash. The first portion of the label, which is SSRC, denotes the SSRC columns. The second portion comprises of a letter and number, which refer to the type of strengthening system and CFRP band width. The third portion of the label indicates the load types applied to test the columns. For the SSRC columns subjected to eccentric compression, the third portion includes the letter E and a number presenting the load eccentricity, while the SSRC columns subjected to pure bending, the third portion is a letter B, standing for pure bending. For instance, Column SSRC-B0-E25 is a column of control group (Group SSRC-B0), which had no confinement and was subjected to 25 mm eccentric compression while Column SSRC-B60-B is a column of third group (Group SSRC-B60), which was strengthened with 60 mm CFRP band and subjected to pure bending.

2.2. Material properties

The concrete properties (i.e., compressive strength - f_{co}) were determined in line with the AS 1012.9:2014 [60].

The f'_{co} at the 28-day was 36 MPa, which was the test result of three concrete cylinders, which had a height and diameter of 200 mm and 100 mm, respectively. The engineering properties of steel reinforcement (i.e., tensile strength - f_{sy}) determined in line with AS 1391-2007 [61], are presented in Table 2. The f_{sy} of longitudinal reinforcement (deformed steel bar with 12mm diameter) was 568 MPa and f_{sy} of lateral ties (plain steel bar with 6mm diameter) was 517 MPa. The unidirectional CFRP sheet used to make CFRP bands had a thickness of 0.167 mm. The engineering properties of CFRP (i.e., elastic modulus - E_f ; tensile strain - ϵ_{fu} ; tensile strength - f_{frp}) determined in line with ASTM D3039/D3039M-14 [62] are presented in Table 3.

Table 2. Tensile properties of the steel bars

Bar	Reinforcement	Diameter (mm)	f_{sy} (MPa) ^a	ϵ_y (%)	E (GPa) ^b
N12	Longitudinal	12	568	0.327	173
R6	Transverse	6	517	0.284	182

Table 3. Mechanical properties of one ply CFRP flat coupons

Material	n	t_f (mm)	w_f (mm)	f_{frp} (MPa)	ϵ_{fu} (%)	E_f (GPa)
CFRP	1	0.167	26.12	3729	1.6	240.43

where w_f = Width of coupons

2.3. Test setup and Instrumentation

The high strength plaster was employed for capping the column two ends and attaching the columns with two steel adaptor plates (SAP) to make sure a uniform distribution of the compression loading. A Universal Testing Machine (UTM) with a testing ability of 5 ton was employed for generating the compression loading in testing all the SSRC columns. The concentric compression loading was transferred to the SSRC columns via SAP while the eccentric compression loading was transferred to the SSRC columns via a pair of the SAP connected to the ball joint plates (BJP). The pure bending loading was distributed to the SSRC columns, which behaved as beams, via two steel rigs (SR) placed at the column bottom and top. The details of the SAP, BJP and SR could be found in [23]. The axial and lateral deformation of the SSRC columns happened during the test was recorded by a pair of the Linear Variable Differential Transformer (LVDT) and a laser triangulation, respectively, which were linked to the data loggers for recording the deformation every two seconds. The instruments and test setup can be found in Figure 2.

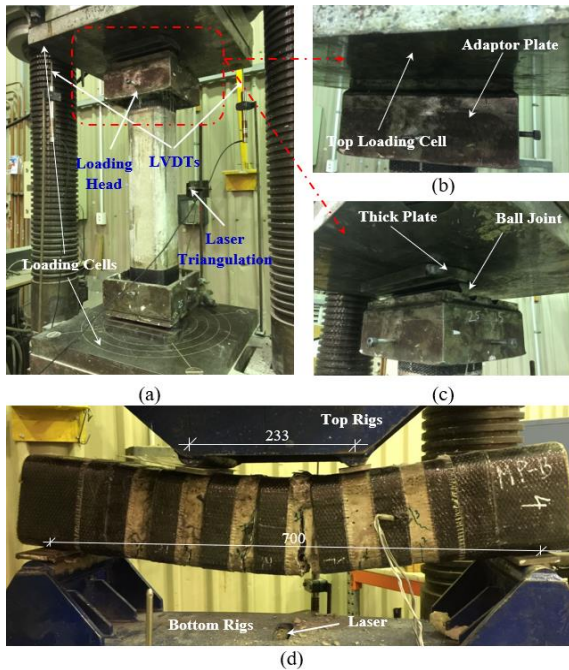


Figure 2. Loading system and instruments: (a) test setup of the EC-SSRC column, (b) loading head system for concentrically loaded specimens, (c) loading head system for eccentrically compressed columns, and (d) test setup of the column under pure bending

The preload and unload procedures were undertaken before officially starting the test to ensure that the test columns were kept straight and stable on the UTM. In fact, the columns were preloaded with 2kN/s loading rate up to 10% of its expected strength and unloaded to 2% of its expected strength before starting the test. After the preload and unload procedures, the official testing of the columns

was carried out with 0.3 mm/min loading rate and ended when the recorded axial load after the peak reduced by 20-30% of the peak load.

3. Experimental results and discussion

3.1. Column failure modes

Figure 3 presents the typical failures of concentrically compressed SSRC (CC-SSRC) columns. Column SSRC-B0-E0 was failed by the cover concrete loss and the longitudinal reinforcement buckling. Unlike Column SSRC-B0-E0, the failure of Columns SSRC-B60-E0 and SSRC-B40-E0 started by cover concrete cracking at the non-strengthened zone and followed by the CFRP band above the mid-column rupture, ended by the longitudinal reinforcement buckling. The CFRP band of Columns SSRC-B60-E0 and SSRC-B40-E0 was ruptured at one of the column corners because of the stress concentration. The CFRP band rupture caused a loud sound. Column SSRC-B40-E0 failure was consistent with the observation from experimental investigation carried out by Triantafyllou, et al. [51] and by Matthys, et al. [46] in which the CFRP bands were placed in between lateral ties and steel helixes, respectively. It should be mentioned here that the level of cover concrete cracking at the non-strengthened zone during the failure period occurred on Column SSRC-B60-E0 was much more severe than that occurred on Column SSRC-B40-E0, which was ascribed to the dual confining pressure of lateral tie at the non-strengthened zone in inhibiting the dilation of the core concrete and postponing the non-strengthened cover concrete cracking.

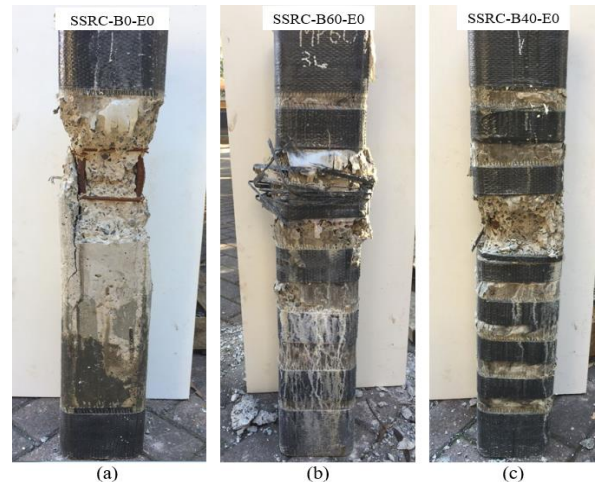


Figure 3. Failure modes of SSRC columns under axial compression: (a) Column SSRC-B0-E0, (b) Column SSRC-B60-E0, and (c) SSRC-B40-E0

Figures 4 and 5 present the typical failures of eccentrically compressed SSRC (EC-SSRC) columns. Columns SSRC-B0-E15 and SSRC-B0-E25 failed by the cover concrete crushing occurred on the compression face at the mid-column vicinity, followed by the hair line cracks in transverse direction of cover concrete on the tension face at the mid-column and the longitudinal reinforcement buckling on the compression face. The failure of Columns SSRC-B60-E15 and SSRC-B60-E25 was characterized by non-strengthened cover concrete crushing occurred on the compression face at the mid-column vicinity, followed by the hair line cracks in transverse direction of concrete in the tension face. The CFRP bands of Columns

SSRC-B60-E15 and SSRC-B60-E25 were not ruptured. The longitudinal reinforcement buckling occurred at the compression face was seen by removing the cover concrete after removing the columns from the testing machine. Unlike Column SSRC-B60-E15, the failure of Column SSRC-B40-E15 was controlled by the CFRP band rupture occurred on the compression face at the mid-column after the crushing of non-strengthened cover concrete in the compression face and the hair line cracks in the tension face in transverse direction. The CFRP band rupture occurred on the compression face of Column SSRC-B40-E15 could be because of the dilation of the core concrete and the longitudinal reinforcement buckling. Similar to other EC-CFRPBC-SSRC, CFRP band rupture was observed at the column corner indicating that the column corners happened stress concentration. Similar Column SSRC-B60-E25, Column SSRC-B40-E25 failed by non-strengthened cover concrete crushing occurred on the compression face and hair line cracks on the tension face in transverse direction without the CFRP band rupture.

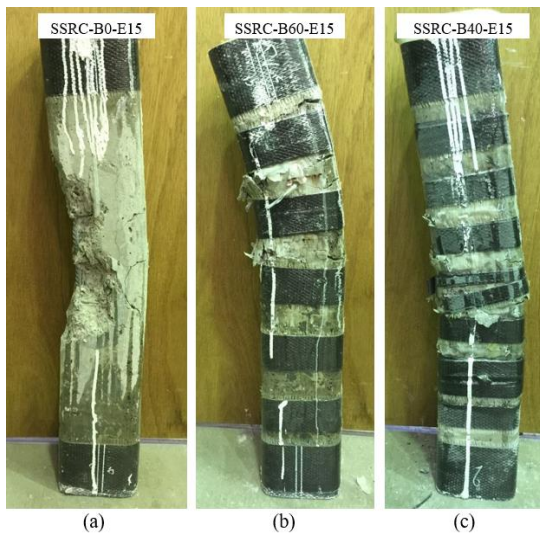


Figure 4. Failure modes of columns tested under 15 mm eccentric compression: (a) Column SSRC-B0-E15, (b) Column SSRC-B60-E15, and (c) Column SSRC-B40-E15

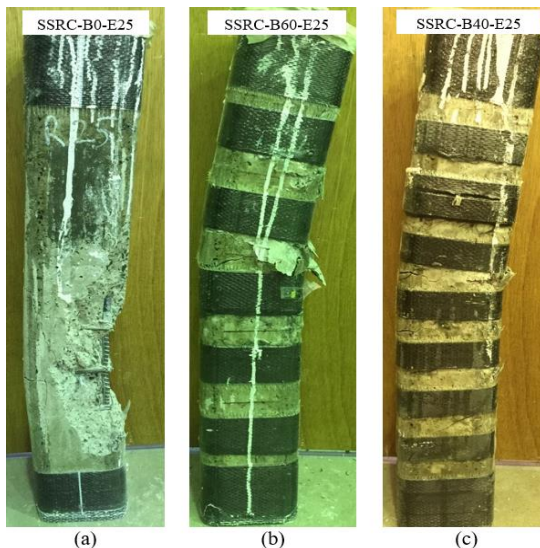


Figure 5. Failure modes of specimens tested under 25 mm eccentric compression: (a) Column SSRC-B0-E25, (b) Column SSRC-B60-E25, and (c) Column SSRC-B40-E25

Figure 6 presents the typical failures of SSRC columns subjected to pure bending of four-point loads. Columns SSRC-B0-B, SSRC-B60-B and SSRC-40-B failed by tensile longitudinal reinforcement break after cover and core concrete at the tension face underwent a wide vertical crack and concrete at the compression face underwent a crushing. Columns SSRC-B0-B, SSRC-B60-B and SSRC-40-B started to be failed by vertical concrete cracks at the tension face due to flexural stresses and quickly extended the cracks to the compression face. The first vertical crack was initiated nearby the midspan for Column SSRC-B0-Band at the non-strengthened zone near by the mid-span for Columns SSRC-B60-B and SSRC-40-B. Unlike Column SSRC-40-B occurring vertical cracks in the zone between two loading points, Columns SSRC-B60-B and SSRC-40-B occurred vertical cracks at non-strengthened zone at the two loading points. After the wide vertical cracks were developed, the crushing of compression concrete was witnessed in the non-strengthened zone for both Columns SSRC-B60-B and SSRC-40-B. In contrast, the crushing of compression concrete was witnessed at the position nearby the loading points for Column SSRC-B0-Band. Next, the rupture of longitudinal reinforcement occurred in Columns SSRC-B0-B, SSRC-B60-B and SSRC-40-B causing an explore sound.

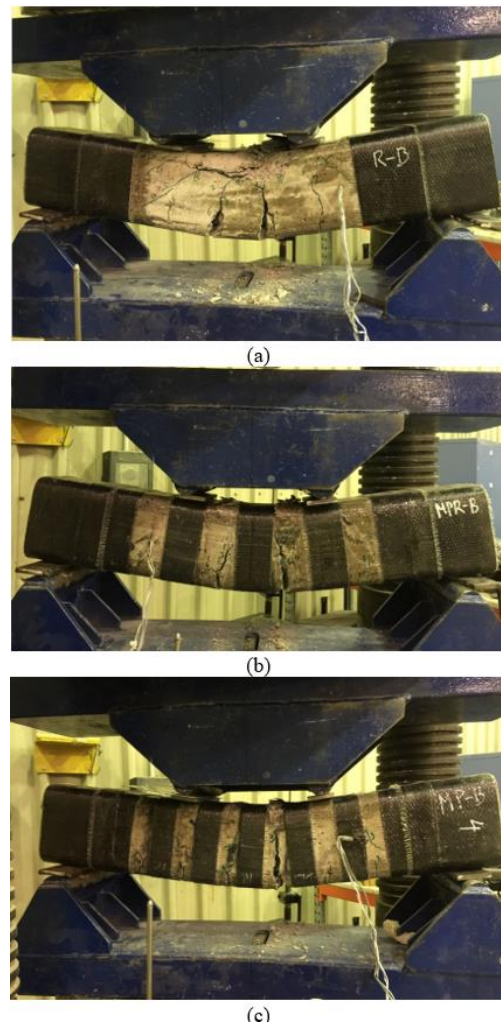


Figure 6. Failure modes of columns tested under four-point bending: (a) Column SSRC-B0-B, (b) Column SSRC-B60-B, and (c) Column SSRC-B40-B

3.2. Behaviour of column specimens

Tables 4 and 5 present, respectively, the key test results of CC-SSRC and EC-SSRC columns. The column ductility (λ) was computed as a ratio of two areas of A_1 and A_2 in which the A_1 was area under the load-deformation relationship up to the ultimate failure load (P_{uf}) and A_2 was the area under the load-deformation relationship up to the yield load (P_y) [30, 42] as:

$$\lambda = \frac{A_1}{A_2} \quad (1)$$

The P_{uf} was determined as the axial load in the post-peak descending portion of the load-deformation relationship, which was equal to 85% of the ultimate load (P_{ult}) [63]. The P_y was the axial load in the pre-peak ascending portion of the load-deformation relationship at the intersection point between two straight lines in which the first one was formed by the point corresponding to 75% of the first peak axial load (P_{peak1}) and the origin, while the second one was the horizontal line passing the P_{peak1} .

The first column of each group was subjected to concentric compression loading and the key test results of CC-SSRC columns is presented in Table 4 while the load-deformation response is presented in Figure 7. The load-deformation response of Columns SSRC-B0-B, SSRC-B60-B and SSRC-B40-B showed the similar ascending portion before concrete cracking, which indicates that external FRP Strengthening had no effect to the response of the SSRC columns before the concrete cracking. However, CFRP strengthening had profound effect on the response of SSRC columns after concrete cracking by providing the lateral confinement in inhibiting the concrete dilation [16, 64], leading to the distinctive post-peak load-deformation response. The post-peak axial load of Column SSRC-B60-E0 and SSRC-B40-E0 underwent a slight reduction and slight rise, respectively; whereas, the post-peak axial load of Column SSRC-B0-E0 experienced an abrupt fall to the P_{uf} . Column SSRC-B0-E0 experienced an abrupt fall of the axial load after reaching the P_{peak1} as cover concrete was spalling which revealed the brittle behaviour of Column SSRC-B0-E0. In contrast, Column SSRC-B60-E0 underwent a slight reduction of the post-peak axial load as non-strength cover concrete was cracked. The cracked cover concrete still attached to the core concrete and supported the column in sustaining the applied load as well as preventing abrupt fall

of the axial load. However, the axial load of Column SSRC-B60-E0 steadily decreased until reaching the P_{uf} because the confinement effect of CFRP bands was less than the degradation of SSRC column. A similar load-deformation response of CC-FRPBC-SSRC columns was also found in [30]. Unlike Column SSRC-B60-E0, Column SSRC-B40-E0 experienced a slight rise in the axial load after reaching the P_{peak1} because of non-strengthened cover concrete cracking then underwent a steady rise to reach the second peak load (P_{peak2}). The rise in the post-peak axial load of Column SSRC-B40-E0 indicated that the dual confinement provided by lateral ties and CFRP bands at non-strengthened zone was higher than the degradation of SSRC column caused by cover concrete cracking.

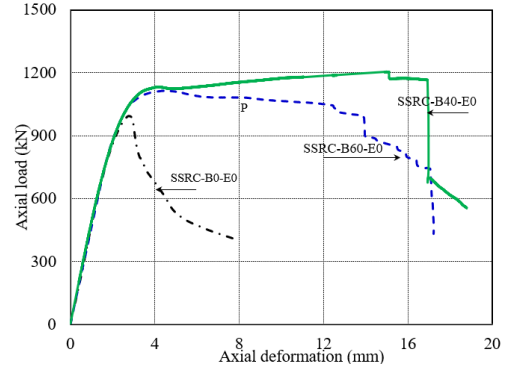


Figure 7. Axial load-deformation relationship of the concentrically compressed columns

The P_{ult} obtained by Column SSRC-B0-E0 was 993.5 kN, which is 12.1% lower than the P_{ult} of Column SSRC-B0-E0. Column SSRC-B40-E0 carried the highest P_{ult} with 8.1% higher than the P_{ult} of Column SSRC-B60-E0 and 21.2% higher than the P_{ult} of Column SSRC-B0-E0. The higher P_{ult} of Columns SSRC-B60-E0 and SSRC-B40-E0 than that of Column SSRC-B0-E0 indicated the effect of CFRP bands in enhancing the strength of SSRC columns. The higher P_{ult} of Column SSRC-B40-E0 compared to Column SSRC-B60-E0 revealed the effect of lateral ties in preventing the dilation of the non-strengthened core concrete and in postponing the non-strengthened cover concrete cracking. The λ of Column SSRC-B60-E0 was 400% higher than the λ of Column SSRC-B0-E0. The λ of Column SSRC-B40-E0 was 561.3% higher than the λ of Column SSRC-B0-E0 and 32.3% higher than the λ of Column SSRC-B0-E0.

Table 4. Experimental results of the concentrically and eccentrically compressed SSRC columns

Column	e	P_y (kN)	Δ_y at P_y (mm)	P_{ult} (kN)	Δ_u at P_{ult} (mm)	δ_y at P_{ult} (mm)	Δ_{ult} at P_{uf} (mm)	λ
SSRC-B0-E0		902	2.17	993.5	2.76	-	3.15	1.86
SSRC-B60-E0	0	990	2.46	1114.2	4.18	-	14.25	9.3
SSRC-B40-E0		1004	2.55	1204.4	14.9	-	16.96	12.3
SSRC-B0-E15		687	1.93	731.8	2.24	2.46	2.41	1.48
SSRC-B60-E15	15	733.2	2.07	802.3	2.8	3.21	5.9	4.51
SSRC-B40-E15		836.4	2.22	905.1	2.92	3.59	5.1	3.45
SSRC-B0-E25		595.4	1.85	630.2	2.19	2.52	2.46	1.61
SSRC-B60-E25	25	665.8	2.08	684.93	2.58	3.42	4.55	3.24
SSRC-B40-E25		683.7	2.31	742.8	3.07	4.7	6.0	3.97

Δ_y = axial deformation at P_y ; Δ_u = axial deformation at P_{ult} ; Δ_{ult} = axial deformation at $0.85P_{ult}$;

A total of six columns (two columns from each group) were tested under eccentric compression loading including three 15 mm eccentrically compressed SSRC columns and three 25 mm eccentrically compressed SSRC columns. Table 4 presents the key test results of eccentrically compressed SSRC columns, while Figures 8 and 9 present the load-deformation and the load-lateral deformation response (hereafter referred as the load-deformation-lateral deformation response for brevity) of 15 mm and 25 mm eccentrically compressed SSRC columns, respectively. In overall, the load-deformation-lateral deformation response of 15 mm and 25 mm eccentrically compressed SSRC columns only experienced the P_{peak1} , which represents the LCC of SSRC columns before the spalling/crushing of non-strengthened cover concrete in the compression face.

Table 5. Experimental results of SSRC columns under pure bending

Column	P_y (kN)	ρ_y at P_y (mm)	P_{ult} (kN)	ρ_u at P_{ult} (mm)	ρ_{ult} at P_{uf} (mm)	λ
SSRC-B0-B	111.08	3.5	126.1	6.11	56.44	27.4
SSRC-B60-B	111.03	3.5	155.9	24.46	36.84	28.1
SSRC-B40-B	126.0	4.1	160.4	32.65	41.4	30.5

Where ρ_y = midspan deformation at P_y ; ρ_u = midspan deformation at P_{ult} ; ρ_{ult} = midspan deformation at P_{uf} ; $P_{uf} = 0.85P_{ult}$

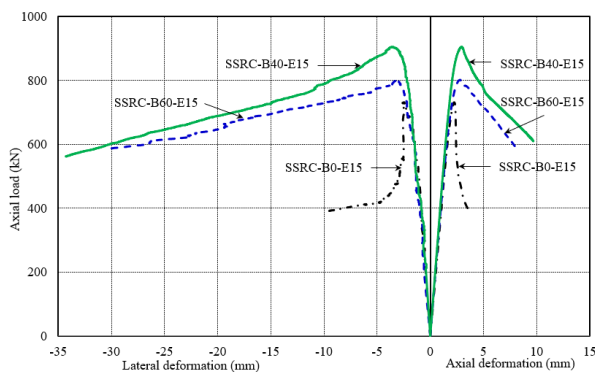


Figure 8. Axial load-deformation-lateral deformation relationship of the 15 mm eccentrically compressed columns (mm)

As illustrated in Figure 8, the ascending portion of the load-deformation-lateral deformation response of Columns SSRC-B0-E15, SSRC-B60-E15 and SSRC-B40-E15 showed similar pattern up to the P_{ult} of the control column (Column SSRC-B0-E15), which indicated the identical stiffness between the SSRC columns before the concrete cracking. After reaching the P_{ult} , Column SSRC-B0-E15 experienced abrupt loss of the axial load to the P_{uf} because of the cover concrete spalling in the compression face. In contrast, the axial load of Columns SSRC-B60-E15 and SSRC-B40-E15 passed the P_{ult} of Column SSRC-B0-E15 then continued to increase to the P_{ult} before decreasing to the P_{uf} progressively. Column SSRC-B40-E15 showed higher stiffness and P_{ult} compared to Column SSRC-B60-E15 after passing the P_{ult} of Column SSRC-B0-E15, which was ascribed to the confinement effect of lateral ties in the compression face of Column SSRC-B40-E15. It should be mentioned that the gradient of the post-peak load-deformation-lateral deformation response of Column SSRC-B40-E15 was slightly higher than those of Column SSRC-

B60-E15 resulted from CFRP band rupture in the mid-height of the Column SSRC-B40-E15. Unlike Column SSRC-B40-E15, there was no rupture of CFRP band occurred.

The highest P_{ult} was carried by Column SSRC-B40-E15 (905.1 kN), followed by Column SSRC-B60-E15 (802.3 kN) and Column SSRC-B0-E15 (731.8 kN). The P_{ult} of Column SSRC-B60-E15 was 9.6% higher than the P_{ult} of Column SSRC-B0-E15. The P_{ult} of Column SSRC-B40-E15 was 12.9% and 23.7% higher than the P_{ult} of Columns SSRC-B60-E15 and SSRC-B0-E15, respectively. The λ of Column SSRC-B60-E15 was 204.7% higher than the λ of Column SSRC-B0-E15. The λ of Column SSRC-B40-E15 was 23.5% lower than the λ of Column SSRC-B60-E15 and 132.7% higher than the λ of Column SSRC-B0-E15. The lower ductility of Column SSRC-B40-E15 compared to Column SSRC-B60-E15 was due to the higher slope of post-peak axial load of Column SSRC-B40-E15, which was resulted from CFRP band rupture at the mid-column.

Figure 9 presents the load-deformation-lateral deformation response of 25 mm eccentrically compressed SSRC columns. The post-peak load-deformation of Columns SSRC-B60-E25 and SSRC-B40-E25 showed similar pattern with the gradual reduction of the axial load, whereas the post-peak load-deformation of Column SSRC-B0-E25 showed an immediate loss of axial load after attaining the P_{ult} . The higher P_{ult} and the steady reduction of the axial load of Columns SSRC-B60-E25 and SSRC-B40-E25 after the P_{ult} compared to those of Column SSRC-B0-E25 illustrated the confinement effect of CFRP bands in preventing the sudden spalling of cover concrete in the compression face.

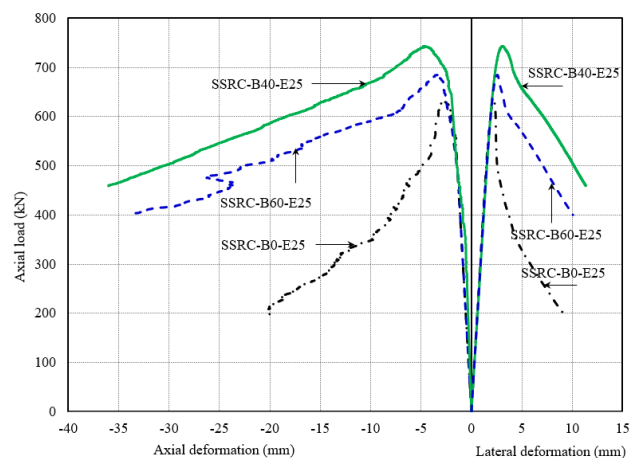


Figure 9. Axial load-deformation-lateral deformation relationship of the 15 mm eccentrically compressed columns (mm)

Column SSRC-B0-E25 sustained the lowest P_{ult} of 683.7 kN, which was 8.6% lower than the P_{ult} of Column SSRC-B60-E25 (684.9 kN) and 17.9% lower than the P_{ult} of Column SSRC-B40-E25 (742.8 kN), respectively. The P_{ult} of Column SSRC-B40-E25 was 8.5% higher than the P_{ult} of Column SSRC-B60-E25. The higher P_{ult} of Column SSRC-B40-E25 compared to Column SSRC-B60-E25 was because of higher confining pressure generated by lateral ties at the non-strengthened zone of Column SSRC-B40-E25 leading to the later cracking and no-spalling of non-

strengthened cover concrete in the compression face. The λ of Column SSRC-B40-E25 was 22.5% higher than the λ of Column SSRC-B60-E25 and 146% higher than the λ of Column SSRC-B0-E25. Unlike to Column SSRC-B40-E15, the post-peak axial load of Column SSRC-B40-E25 had the similar pattern as the post-peak axial load of Column SSRC-B60-E25 because of no rupture of CFRP band occurred on Columns SSRC-B40-E25 and SSRC-B60-E25. The λ of Column SSRC-B60-E25 was 101.2% higher than the λ of Column SSRC-B0-E25. The higher ductility of Columns SSRC-B60-E25 and SSRC-B40-E25 compared to Column SSRC-B0-E25 was ascribed to the progressive reduction of the post-peak load-deformation of Columns SSRC-B60-E25 and SSRC-B40-E25. Table 5 presents the key test results of SSRC columns under pure bending, while Figure 10 presents the flexural load-midspan deflection (hereafter referred as flexural load-deflection) response of SSRC columns under pure bending. The ascending portion of the flexural load-deflection response of Columns SSRC-B0-B, SSRC-B60-B and SSRC-B40-B was similar up to the yield flexural load (P_y^*) of Columns SSRC-B0-B. Columns SSRC-B60-B and SSRC-B40-B experienced the ascending post-peak flexural load-deflection response, whereas Column SSRC-B0-B experienced the linear post-peak flexural load-deflection response. The higher ultimate flexural load (P_{ult}^*) and the post-peak ascending flexural load-deflection response of the CFRP confined SSRC columns were also reported in [3], [23], [28]. This could be ascribed to the CFRP confinement effect on the concrete of compression face the CFRP confined columns after tensile longitudinal reinforcement yielding. The contribution of compressive concrete strength on the P_{ult}^* (the ultimate moment) of non-strengthened under-reinforced column was insignificant [27]. The linear post-peak flexural load-deflection of Column SSRC-B0-B was due to the yielding of tensile longitudinal reinforcement. A similar observation of the linear post-peak flexural load-deflection of control SSRC column was reported in [28].

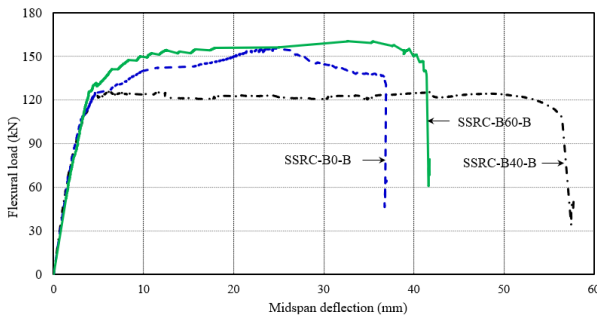


Figure 10. Load-midspan deflection relationship of columns under four-point bending (mm)

The P_{ult}^* of Columns SSRC-B60-B (155.9 kN) and SSRC-B40-B (160.4 kN) was 23.6% and 27.2% higher than the P_{ult}^* of Column SSRC-B0-B, respectively. The P_{ult}^* of Column SSRC-B40-B was closed to the P_{ult}^* of Column SSRC-B60-B with 2.9% difference. The λ of Column SSRC-B60-B and Column SSRC-B40-B was 2.6% and 11.4% higher than the λ of Column SSRC-B0-B, respectively. The λ of Column SSRC-B40-B was 8.5% higher than the λ of Column SSRC-B60-B.

3.3. Effect of load eccentricity (e)

As illustrated in Table 4, the higher e , the lower LCC and λ of the SSRC columns. The reduction of the LCC and λ of the SSRC columns resulting from the increase of the e was due to the reduction of compression area confined by CFRP. It is noted that the increase of the e from 15 mm to 25 mm resulted in the increase in the λ of Column SSRC-B40-E15, which was due to the abrupt loss of the axial load of Column SSRC-B40-E15 compared to the steady reduction of the axial load of Column SSRC-B40-E25. The abrupt loss of the axial load of Column SSRC-B40-E15 was resulted from CFRP band rupture, whereas, the steady decrease of the axial load of Column SSRC-B40-E25 resulted from cover concrete cracking in the compression ace without any CFRP band rupture.

4. Axial and flexural interaction diagrams (strength diagram)

Figure 11 shows the experimental axial-flexural interaction (P-M) diagrams of SSRC columns, plotted based on four points in which the first point presents the column LCC under concentric compression. The second and third points present the P_{ult} and bending moment (M_{ult}) of the SSRC columns tested under 15 mm and 25 mm eccentric compression, respectively. The experimental M_{ult} at the mid-column of CC-SSRC column was given using Eq. (2). The fourth point presents the pure bending moment of column under four-point flexural load. The M_u at the midspan of column was given using Eq. (3).

$$M_{ult} = P_{ult}(e + \delta) \quad (2)$$

$$M_{ult} = \frac{1}{2}P_{ult}L \quad (3)$$

where δ indicates the column lateral deformation at the P_{ult} and L indicate the distance between two supports of the test column, which is 233 mm.

As illustrated in Figure 11, the increase of the M_{ult} of SSRC columns was corresponding to the decrease of the P_{ult} . Columns of Groups SSRC-B0, SSRC-B60 and SSRC-B60 showed the similar experimental axial-flexural behaviour under concentric and eccentric compression. The discrepancy of the axial-flexural behaviour of the columns of Groups SSRC-B0, SSRC-B60 and SSRC-B60 under pure bending may be ascribed to non-pure bending of columns because of the short of span-to-depth ratio of the columns. However, under all loading condition, Group SSRC-B40 columns always showed the highest P_{ult} and highest M_{ult} , followed by Group SSRC-B60 columns and Group SSRC-B0 columns. Under 15 mm and 25 mm eccentric compression, the M_{ult} of Columns SSRC-B60-E15 and SSRC-B60-E25 were 14.1% and 12.5% higher than the M_{ult} of Columns SSRC-B0-E15 and SSRC-B0-E25, respectively. The M_{ult} of columns SSRC-B40-E15 and SSRC-B40-E25 were 15% and 13.3% higher than the M_{ult} of Columns SSRC-B60-E15 and SSRC-B60-E25 and 31.3% and 27.5% higher than the M_{ult} of Columns SSRC-B0-E15 and SSRC-B0-E25. For pure bending, the M_{ult} of Column SSRC-B60-B was 23.5% higher than the M_{ult} of Column SSRC-B0-B. The M_{ult} of Column SSRC-B40-B was 3% higher than the M_{ult} of Column SSRC-B60-B and

27.1% higher than the M_{ult} of Column SSRC-B0-B. The higher P_{ult} and M_{ult} of the columns of Groups SSRC-B60 and SSRC-B40 compared to those of the columns of Group SSRC-B0 indicated the efficiency of discontinuous FRP strengthening in improving the performance of SSRC columns.

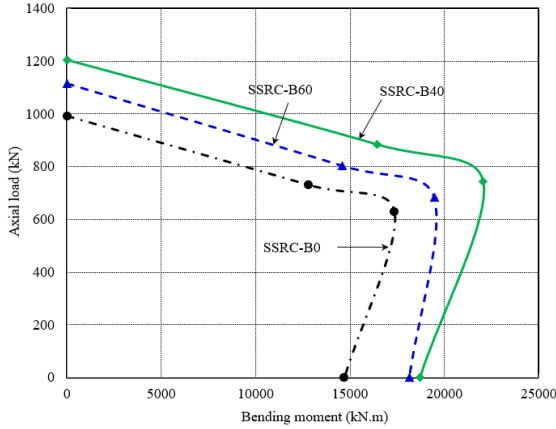


Figure 11. Experimental axial-flexural interaction diagrams

The theoretical P-M diagrams were established based on equivalent stress block in accordance with AS 3600:2009 [65], which is relied on an assumption of strain compatibility and force equilibrium and then compared with the experimental P-M diagrams. The theoretical P-M diagram was plotted based on four points, which is corresponding to four points of the experimental P-M diagram. It should be mentioned that the theoretical P-M diagrams of CFRPBC-SSRC columns were constructed similarly to the theoretical P-M diagram of unconfined

SSRC columns; however, the stress and strain of FRP confined concrete was employed instead of the stress and strain of unconfined concrete.

The theoretical P_{ult} of CFRPBC-SSRC columns under concentric compression was calculated in accordance with ACI 440.2R-17 [2], as illustrated in Eq. (4)

$$P_{ult} = 0.85f'_{cc}(A_g - A_s) + f_{sy}A_s \quad (4)$$

where f'_{cc} stands for the FRP confined concrete strength, A_g and A_s stand for the gross cross-sectional area of column and longitudinal reinforcement; respectively and f_{sy} stands for the longitudinal reinforcement yield strength.

The compressive strength (f'_{cc}) and strain (ϵ_{cc}) of FRP confined concrete were computed based on two distinguished codes including ACI 440.2R-17 [2] and FIB Bulletin 14 [54]. In FIB Bulletin 14 [54], the lower confinement effect of discontinuous strengthening was taken into account by introducing a confinement effectiveness coefficient (k_e), which was adopted from the k_e proposed by Mander, et al. [66] in calculating effective lateral confining pressure (f_l) of lateral ties. In contrast, ACI 440.2R-17 [2] has not yet included partial wrapping, thus, there has no k_e proposed. Therefore, when applying the code of ACI 440.2R-17 [2] for calculating the strength of CFRPBC-SSRC columns, the k_e proposed in FIB Bulletin 14 [54] was adopted for considering the lower confinement effect of discontinuous strengthening in comparison to continuous strengthening. The f'_{cc} and ϵ_{cc} of FRP confined concrete were calculated based on the equations presented in Table 6.

Table 6. Equations of ACI 440-2R and FIB Bulletin 14

ACI 440.2R-17 [1]	FIB Bulletin 14 [2]
$\frac{f'_{cc}}{f'_{co}} = 1 + \omega_f 3.3k_a \frac{f_l}{f'_{co}} = 1 + 3.135k_a \frac{f_l}{f'_{co}}$ $\epsilon_{cu} = \epsilon_{co} \left[1.5 + 12k_b \left(\frac{f_l}{f'_{co}} \right) \left(\frac{\epsilon_{fe}}{\epsilon_{co}} \right)^{0.45} \right]$ $0.02 \left[1.5 + 12k_b \left(\frac{f_l}{f'_{co}} \right) \left(\frac{\epsilon_{fe}}{\epsilon_{co}} \right)^{0.45} \right]$ $f_l = \frac{2E_f n \epsilon_{fe} t_f}{D} k_e$ $\epsilon_{fe} = k_e \epsilon_f = 0.55 \epsilon_f$ $k_a = \frac{A_e}{A_c} \left(\frac{b}{h} \right)^2; k_b = \frac{A_e}{A_c} \left(\frac{h}{b} \right)^{0.5}$ $\frac{A_e}{A_c} = \left(\frac{1 - \left(\frac{b}{h} \right) (h - 2r_c)^2 + \left(\frac{h}{b} \right) (b - 2r_c)^2}{(1 - \rho_s)} \right) / (3A_g - \rho_s)$ $D = \sqrt{h^2 + b^2}$	$f'_{cc} = f'_{co} \left(0.2 + 3 \sqrt{\frac{f_{l,eff}}{f'_{co}}} \right)$ $\epsilon_{cc} = \epsilon_{co} \left(2 + 1.25 \frac{E_c \epsilon_{fe}}{f'_{co}} \sqrt{\frac{f_{l,eff}}{f'_{co}}} \right)$ $f_l = \frac{1}{2} \rho_f E_f \epsilon_{fe} k_e k_a$ $\rho_f = \frac{4t_f}{d_f}$ $E_c = 4700 \sqrt{f'_{co}}$ $k_a = \left[1 - \frac{(h - 2r_c)^2 + (b - 2r_c)^2}{3A_c(1 - \rho_s)} \right]$ $k_e = \frac{\left(1 - \frac{s'}{2d_f} \right)^2}{1 - \rho_{sg}} \approx \left(1 - \frac{s'}{2d_f} \right)^2$

The experimental and theoretical results presented in Figure 12 indicates that using the models provided in ACI 440.2R-17 [2] in estimating the P_{ult} of CFRPBC-SSRC columns was more accurate compared to using the models provided in FIB Bulletin 14 [54]. The estimation of P_{ult} of

specimens under concentric and eccentric compression using the model provided in ACI 440.2R-17 [2] was conservative. The model provided in FIB Bulletin 14 [54] overestimated the P_{ult} of the CFRPBC-SSRC columns. The lower theoretical M_{ult} compared to experimental M_{ult}

of SSRC columns under pure bending could be due to the non-pure bending of test columns.

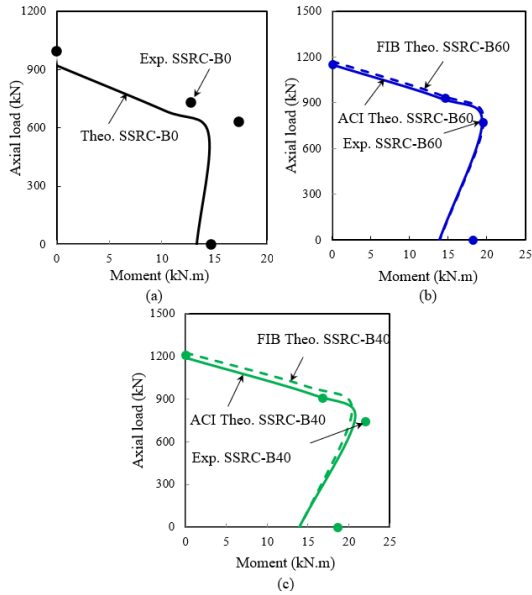


Figure 12. Comparison between the experimental and theoretical P-M diagrams: (a) Group SSRC-B0, (b) Group SSRC-B60, and (c) Group SSRC-B40

5. Conclusions

This investigation examines the effect of the position and width of CFRP bands on the performance of eccentrically compressed CFRP band-confined SSRC columns by testing four control SSRC columns and eight CFRP band-confined SSRC columns. The key parameters consider in this investigation consisting of different discontinuous strengthening schemes (non-strengthening, discontinuous strengthening without considering the position of lateral ties and discontinuous strengthening with CFRP bands placed in between lateral ties) and the magnitude of the applied load eccentricity. Based on the observation and test findings, the main conclusions are as follows:

(1) The SSRC columns sustained higher strength by discontinuously confined with CFRP bands compared to their counterparts without CFRP strengthening. Under concentric, eccentric axial compression (15 mm and 25 mm eccentricity) and pure bending, the strength of the SSRC columns discontinuously confined with CFRP band without taking into account the position of the lateral ties was 12.1%, 9.6%, 8.6% and 23.6%, respectively, higher than that of their counterparts without CFRP confinement, while the improvement of strength of SSRC columns discontinuously confined with CFRP bands placed in between lateral ties was 21.2%, 23.7%, 17.9% and 27.2%.

(2) At the same amount of CFRP utilized for discontinuous confinement of SSRC columns, employing smaller CFRP bands and placing CFRP bands between lateral ties resulted in better performance of CFRP band-confined SSRC columns compared to placing CFRP bands without taking into account the position of lateral ties. The differences between the strength of discontinuous confinement with and without considering the position of lateral ties under concentric, eccentric axial compression

(15 mm and 25 mm eccentricity) and pure bending were 8.1%, 9.6%, 8.6% and 8.5%, respectively.

(3) The SSRC columns achieved a remarkable enhancement of the ductility by discontinuously strengthening with CFRP bands. The ductility of the SSRC columns discontinuously confined with CFRP bands without taking into account the position of the lateral ties was much lower than that of their counterparts discontinuously confined with CFRP bands in placed in between the lateral ties.

(4) The experimental compressive strength-bending moment capacity of SSRC columns discontinuously confined with CFRP bands placed in between lateral ties was higher than that of their counterparts confined with CFRP bands without taking into account the position of lateral ties. The compressive strength-bending moment capacity of CFRP band-confined SSRC columns was higher than that of SSRC columns without CFRP strengthening.

(5) The theoretical compressive and flexural strength of CFRP band-confined SSRC columns determined based on the adoption of confinement effectiveness coefficient and ACI 440.2R-17 [2] model was in good agreement with the test results.

(6) The ACI 440.2R-17 [2] model was found to be more accurate in estimating the compressive and flexural strength of CFRP band-confined SSRC columns, whereas, the FIB Bulletin 14 [54] model was found to overestimate ultimate compressive and flexural strength of CFRP band-confined SSRC columns.

Acknowledgements: The first three authors express sincere acknowledgements to The Murata Science Foundation and The University of Danang - The University of Science and Technology for providing a financial support to this study through the T2022-02-09MSF project.

Notations

- f'_{cc} = maximum compressive strength of FRP confined concrete;
- f_l = lateral confining pressure generated by FRP jacket;
- f'_{co} = compressive strength of unconfined concrete;
- ϵ_{cu} = ultimate axial compressive strain of confined concrete;
- ϵ_{co} = maximum compressive strain of unconfined concrete;
- ϵ_{fe} = effective strain of FRP;
- E_f = tensile modulus of elasticity of FRP;
- ϵ_f = tensile strain of FRP;
- t_f = nominal thickness of one ply of FRP;
- n = number of FRP plies;
- ρ_f = volumetric ratio of FRP jacket;
- k_a = efficiency factor accounting for the geometry of the section in calculating the ultimate axial strength;
- k_b = efficiency factor accounting for the geometry of the section in calculating the ultimate axial strain;
- k_e = efficiency factor accounting for the discontinuous confinement;
- b = short-side dimension of the cross-section;
- h = long-side of the dimension of the cross-section;

r_c = corner radius;
 D = equivalent diameter of cross-section;
 A_e = effectively confined cross-sectional area;
 A_c = cross-sectional area of concrete;
 ρ_s = ratio of longitudinal steel reinforcement;
 E_{cc} = secant modulus of elasticity of FRP confine concrete;
 E_c = initial tangent modulus of elasticity of concrete;
 β = constant coefficient representing the concrete properties;
 d_f = minimum dimension of cross-section;
 s' = clear spacing between transverse FRP bands.

REFERENCES

- [1] J. G. Teng and L. Lam, "Compressive behavior of carbon fiber reinforced polymer-confined concrete in elliptical columns", *J. Struct. Eng.*, vol. 128, no. 12, pp. 1535-1543, 2002, doi: 10.1061/(ASCE)0733-9445.
- [2] ACI Committee 440, "Guide for the Design and Construction of Externally Bonded FRP Systems for Strengthening Concrete Structures", ACI (American Concrete Institute), 2017.
- [3] M. N. S. Hadi, M. T. Jameel, and M. N. Sheikh, "Behavior of Circularized Hollow RC Columns under Different Loading Conditions", *J. Compos. Constr.*, vol. 21, no. 5, p. 04017025, 2017, doi: 10.1061/(ASCE)CC.1943-5614.0000808.
- [4] J. G. Teng, J. F. Chen, S. T. Smith, and L. Lam, *FRP-strengthened RC structures*. UK: John Wiley & Sons, LTD, 2002.
- [5] H. Erdogan, P. Zohrevand, and A. Mirmiran, "Effectiveness of externally applied CFRP stirrups for rehabilitation of slab-column connections", *J. Compos. Constr.*, vol. 17, no. 6, p. 04013008, 2013, Art no. 04013008, doi: 10.1061/(ASCE)CC.1943-5614.0000389.
- [6] H. A. Toutanji, "Stress-strain characteristics of concrete columns externally confined with advanced fiber composite sheets", *ACI Mater. J.*, vol. 96, no. 3, pp. 397-404, 1999.
- [7] G. Campione, "Influence of FRP wrapping techniques on the compressive behavior of concrete prisms", *Cem. Concr. Compos.*, vol. 28, no. 5, pp. 497-505, 2006, doi: 10.1016/j.cemconcomp.2006.01.002.
- [8] T. E. Maaddawy, "Strengthening of Eccentrically Loaded Reinforced Concrete Columns with Fiber-Reinforced Polymer Wrapping System: Experimental Investigation and Analytical Modeling", *J. Compos. Constr.*, vol. 13, no. 1, pp. 13-24, 2009, doi: 10.1061/(ASCE)1090-0268(2009)13:1(13).
- [9] L. Lam and J. G. Teng, "Design-oriented stress-strain model for FRP-confined concrete", *Constr. Build. Mater.*, vol. 17, no. 6-7, pp. 471-489, 2003, doi: 10.1016/S0950-0618(03)00045-X.
- [10] M. N. S. Hadi, "Behaviour of FRP wrapped normal strength concrete columns under eccentric loading", *Compos. Struct.*, vol. 72, no. 4, pp. 503-511, 2006, doi: 10.1016/j.compstruct.2005.01.018.
- [11] Y. Wu and Y. Zhou, "Unified Strength Model Based on Hoek-Brown Failure Criterion for Circular and Square Concrete Columns Confined by FRP", *J. Compos. Constr.*, vol. 14, no. 2, pp. 175-184, 2010, doi: 10.1061/(ASCE)CC.1943-5614.0000062.
- [12] K. H. Tan, "Strength enhancement of rectangular reinforced concrete columns using fiber-reinforced polymer", *J. Compos. Constr.*, vol. 6, no. 3, pp. 175-183, 2002, doi: 10.1061/(ASCE)1090-0268(2002)6:3(175).
- [13] T. Jiang and J. G. Teng, "Behavior and design of slender FRP-confined circular RC columns", *J. Compos. Constr.*, vol. 17, no. 4, pp. 443-453, 2013, doi: 10.1061/(ASCE)CC.1943-5614.0000333.
- [14] D. Y. Wang, Z. Y. Wang, S. T. Smith, and T. Yu, "Size effect on axial stress-strain behavior of CFRP-confined square concrete columns", *Constr. Build. Mater.*, vol. 118, pp. 116-126, 2016, doi: https://doi.org/10.1016/j.conbuildmat.2016.04.158.
- [15] Z. Wang, D. Wang, S. T. Smith, and D. Lu, "CFRP-confined square RC columns. I: Experimental investigation", *J. Compos. Constr.*, vol. 16, no. 2, pp. 150-160, 2012, doi: 10.1061/(ASCE)CC.1943-5614.0000245.
- [16] J. G. Teng and L. Lam, "Behavior and modeling of fiber reinforced polymer-confined concrete", *J. Struct. Eng.*, vol. 130, no. 11, pp. 1713-1723, 2004, doi: 10.1061/(ASCE)0733-9445(2004)130:11(1713).
- [17] O. Chaallal, M. Shahawy, and M. Hassan, "Performance of axially loaded short rectangular columns strengthened with carbon fiber-reinforced polymer wrapping", *J. Compos. Constr.*, vol. 7, no. 3, pp. 200-208, 2003, doi: 10.1061/(ASCE)1090-0268(2003)7:3(200).
- [18] L. Lam and J. G. Teng, "Design-oriented stress-strain model for FRP-confined concrete in rectangular columns", *J. Reinf. Plast. Compos.*, vol. 22, no. 13, pp. 1149-1186, 2003.
- [19] L. M. Wang and Y. F. Wu, "Effect of corner radius on the performance of CFRP-confined square concrete columns: Test", *Eng. Struct.*, vol. 30, no. 2, pp. 493-505, 2008, doi: 10.1016/j.engstruct.2007.04.016.
- [20] S. P. Tastani, S. J. Pantazopoulou, D. Zdoumba, V. Plakantaras, and E. Akritidis, "Limitations of FRP jacketing in confining old-type reinforced concrete members in axial compression", *J. Compos. Constr.*, vol. 10, no. 1, pp. 13-25, 2006, doi: 10.1061/(ASCE)1090-0268(2006)10:1(13).
- [21] M. N. S. Hadi, "Comparative study of eccentrically loaded FRP wrapped columns", *Compos. Struct.*, vol. 74, no. 2, pp. 127-135, 2006.
- [22] M. N. S. Hadi, "Behaviour of FRP strengthened concrete columns under eccentric compression loading", *Composite Structures*, vol. 77, no. 1, pp. 92-96, 2007, doi: 10.1016/j.compstruct.2005.06.007.
- [23] M. N. S. Hadi and I. B. R. Widiarsa, "Axial and flexural performance of square RC columns wrapped with CFRP under eccentric loading", *J. Compos. Constr.*, vol. 16, no. 6, pp. 640-649, 2012, doi: 10.1061/(ASCE)CC.1943-5614.0000301.
- [24] M. N. S. Hadi, T. M. Pham, and X. Lei, "New Method of Strengthening Reinforced Concrete Square Columns by Circularizing and Wrapping with Fiber-Reinforced Polymer or Steel Straps", *J. Compos. Constr.*, vol. 17, no. 2, pp. 229-238, 2013, doi: 10.1061/(ASCE)CC.1943-5614.0000335.
- [25] A. Saljoughian and D. Mostofinejad, "Corner Strip-Batten Technique for FRP-Confinement of Square RC Columns under Eccentric Loading", *J. Compos. Constr.*, vol. 20, no. 3, p. 04015077, 2016, doi: 10.1061/(ASCE)CC.1943-5614.0000644.
- [26] A. Rahai and H. Akbarpour, "Experimental investigation on rectangular RC columns strengthened with CFRP composites under axial load and biaxial bending", *Compos. Struct.*, vol. 108, no. 1, pp. 538-546, 2014.
- [27] R. F. Warner, S. J. Foster, and A. E. Kilpatrick, *Reinforced Concrete Basics: Analysis and design of reinforced concrete structures. Sydney NSW 2086*, Australia: Pearson Education Australia, 2007.
- [28] T. M. Pham, L. V. Doan, and M. N. S. Hadi, "Strengthening square reinforced concrete columns by circularisation and FRP confinement", *Constr. Build. Mater.*, vol. 49, pp. 490-499, 2013, doi: 10.1016/j.conbuildmat.2013.08.082.
- [29] M. N. S. Hadi and J. Youssef, "Experimental investigation of GFRP-reinforced and GFRP-encased square concrete specimens under axial and eccentric load, and four-point bending test", *J. Compos. Constr.*, vol. 20, no. 5, p. 04016020, 2016, Art no. 04016020, doi: 10.1061/(ASCE)CC.1943-5614.0000675.
- [30] A. Saljoughian and D. Mostofinejad, "Axial-flexural interaction in square RC columns confined by intermittent CFRP wraps", *Compos. Part B: Eng.*, vol. 89, pp. 85-95, 2016, doi: 10.1016/j.compositesb.2015.10.047.
- [31] J. Li and M. N. S. Hadi, "Behaviour of externally confined high-strength concrete columns under eccentric loading", *Compos. Struct.*, vol. 62, no. 2, pp. 145-153, 2003, doi: 10.1016/S0263-8223(03)00109-0.
- [32] M. N. S. Hadi and J. Li, "External reinforcement of high strength concrete columns", *Compos. Struct.*, vol. 65, no. 3-4, pp. 279-287, 2004, doi: 10.1016/j.compstruct.2003.11.003.
- [33] L. Bisby and M. Ranger, "Axial-flexural interaction in circular FRP-confined reinforced concrete columns", *Constr. Build. Mater.*, vol. 24, no. 9, pp. 1672-1681, 2010, doi: 10.1016/j.conbuildmat.2010.02.024.
- [34] D. Mostofinejad and E. Ilia, "Confining of square RC columns with FRP sheets using corner strip-batten technique", *Constr. Build. Mater.*, vol. 70, pp. 269-278, 2014, doi: 10.1016/j.conbuildmat.2014.07.073.
- [35] S. Pessiki, K. A. Harries, K. J. T., R. Sause, and J. M. Ricles, "Axial

- Behavior of Reinforced Concrete Columns Confined with FRP Jackets", *J. Compos. Constr.*, vol. 5, no. 4, pp. 237-245, 2001, doi: 10.1061/(ASCE)1090-0268(2001)5:4(237).
- [36] X. Yang, J. Wei, A. Nanni, and L. R. Dharani, "Shape Effect on the Performance of Carbon Fiber Reinforced Polymer Wraps", *J. Compos. Constr.*, vol. 8, no. 5, pp. 444-451, 2004, doi: 10.1061/(ASCE)1090-0268(2004)8:5(444).
- [37] M. H. Harajli, "Axial stress-strain relationship for FRP confined circular and rectangular concrete columns", *Cem. Concr. Compos.*, vol. 28, no. 10, pp. 938-948, 2006, doi: 10.1016/j.cemconcomp.2006.07.005.
- [38] P. Rochette and P. Labossière, "Axial testing of rectangular column models confined with composites", *J. Compos. Constr.*, vol. 4, no. 3, pp. 129-136, 2000, doi: 10.1061/(ASCE)1090-0268(2000)4:3(129).
- [39] J. H. J. Kim, S. T. Yi, S. H. Lee, S. K. Park, and J. K. Kim, "Compressive behaviour of CFS strengthened concrete specimens with various cross-sectional shapes and laminations", *Mag. Concr. Res.*, vol. 55, no. 5, pp. 407-418, 2003, doi: 10.1680/macrc.55.5.407.37592.
- [40] J. J. Zeng, Y. C. Guo, W. Y. Gao, J. Z. Li, and J. H. Xie, "Behavior of partially and fully FRP-confined circularized square columns under axial compression", *Constr. Build. Mater.*, vol. 152, pp. 319-332, 2017, doi: 10.1016/j.conbuildmat.2017.06.152.
- [41] A. Darby, R. Coonan, T. Ibell, and M. Evernden, "FRP confined square columns under concentric and eccentric loading", in *Advanced Composites in Construction 2011, ACIC 2011 - Proceedings of the 5th International Conference*, 2011, pp. 264-275.
- [42] T. E. Maaddawy, M. E. Sayed, and B. Abdel-Magid, "The effects of cross-sectional shape and loading condition on performance of reinforced concrete members confined with Carbon Fiber-Reinforced Polymers", *Mater. Des.*, vol. 31, no. 5, pp. 2330-2341, 5// 2010. [Online]. Available: <http://www.sciencedirect.com/science/pii/S0261306909006943>
- [43] T. E. Maaddawy, "Behavior of corrosion-damaged RC columns wrapped with FRP under combined flexural and axial loading", *Cem. Concr. Compos.*, vol. 30, no. 6, pp. 524-534, 2008.
- [44] A. Parvin and W. Wang, "Behavior of FRP jacketed concrete columns under eccentric loading", *J. Compos. Constr.*, vol. 5, no. 3, pp. 146-152, 2001, doi: 10.1061/(ASCE)1090-0268(2001)5:3(146).
- [45] W. M. Hassan, O. A. Hodhod, M. S. Hilal, and H. H. Bahnasaway, "Behavior of eccentrically loaded high strength concrete columns jacketed with FRP laminates", *Constr. Build. Mater.*, vol. 138, pp. 508-527, 2017, doi: 10.1016/j.conbuildmat.2017.02.016.
- [46] S. Matthys, H. Toutanji, K. Audenaert, and L. Taerwe, "Axial load behavior of large-scale columns confined with fiber-reinforced polymer composites", *ACI Struct. J.*, vol. 102, no. 2, pp. 258-267, 2005. [Online]. Available: <Go to ISI>://WOS:000227277100009.
- [47] O. A. Hodhod, W. Hassan, M. S. Hilal, and H. Bahnasawy, "Strength and ductility of biaxially loaded high strength RC short square columns wrapped with GFRP jackets", *Struct. Eng. Mech.*, vol. 20, no. 6, pp. 727-745, 2005, doi: 10.12989/sem.2005.20.6.727.
- [48] W. M. Hassan, O. A. Hodhod, M. S. M. Hilal, and H. H. Bahnasawy, "Behavior of high strength concrete columns subjected to small biaxial eccentricity and strengthened by FRP laminates", *ACI Spec. Public.*, no. 293 SP, pp. 111-132, 2012.
- [49] F. Colomb, H. Tobbi, E. Ferrier, and P. Hamelin, "Seismic retrofit of reinforced concrete short columns by CFRP materials", *Compos. Struct.*, vol. 82, no. 4, pp. 475-487, 2008, doi: 10.1016/j.compstruct.2007.01.028.
- [50] H. Saadatmanesh, M. R. Ehsani, and M. W. Li, "Strength and ductility of concrete columns externally reinforced with fiber composite straps", *ACI Struct. J.*, vol. 91, no. 4, pp. 434-447, 1994.
- [51] G. G. Triantafyllou, T. C. Rousakis, and A. I. Karabinis, "Axially Loaded Reinforced Concrete Columns with a Square Section Partially Confined by Light GFRP Straps", *J. Compos. Constr.*, vol. 19, no. 1, p. 04014035, 2015, doi: 10.1061/(ASCE)CC.1943-5614.0000496.
- [52] J. A. O. Barros, D. R. S. M. Ferreira, and R. K. Varma, "CFRP-confined reinforced concrete elements subjected to cyclic compressive loading", *ACI Spec. Public.*, SP-258-6, pp. 85-104, 2007.
- [53] T. W. Park, U. J. Na, L. Chung, and M. Q. Feng, "Compressive behavior of concrete cylinders confined by narrow strips of CFRP with spacing", *Compos Part B-Eng.*, vol. 39, no. 7-8, pp. 1093-1103, 2008, doi: 10.1016/j.compositesb.2008.05.002.
- [54] *Externally bonded FRP reinforcement for RC structures*, FIB Bulletin 14, The International Federation for Structure Concrete, Switzerland, 2001.
- [55] T. C. Rousakis and A. I. Karabinis, "Substandard reinforced concrete members subjected to compression: FRP confining effects", *Mater. Struct.*, vol. 41, no. 9, pp. 1595-1611, 2008, doi: 10.1617/s11527-008-9351-4.
- [56] T. C. Rousakis and A. I. Karabinis, "Adequately FRP confined reinforced concrete columns under axial compressive monotonic or cyclic loading", *Mater. Struct.*, vol. 45, no. 7, pp. 957-975, 2012, doi: 10.1617/s11527-011-9810-1.
- [57] *Building Code Requirements for Structural Concrete*, ACI 318-19, American Concrete Institute, Farmington Hills, MI, 2014.
- [58] A. D. Mai, M. N. Sheikh, and M. N. S. Hadi, "Investigation on the behaviour of partial wrapping in comparison with full wrapping of square RC columns under different loading conditions", *Constr. Build. Mater.*, vol. 168, pp. 153-168, 2018, doi: 10.1016/j.conbuildmat.2018.02.003.
- [59] A. D. Mai, M. N. Sheikh, and M. N. S. Hadi, "Performance evaluation of intermittently CFRP wrapped square and circularised square reinforced concrete columns under different loading conditions", *Struct. Infrastruct. Eng.*, vol. 15, no. 5, pp. 696-710, 2019, doi: 10.1080/15732479.2019.1572201.
- [60] *Methods of testing concrete: Method 9: Compressive strength tests- Concrete, mortar and grout specimens*, AS 1391-2007, Australian Standard, Sydney, NSW, Australia, 2014.
- [61] *Metallic materials-Tensile testing at ambient temperature*, AS 1391-2007, Australian Standard, Sydney, NSW, Australia, 2007.
- [62] *Standard Test Method for Tensile Properties of Polymer Matrix Composite Materials*, D7565/D7565M-10, American Society for Testing and Materials, West Conshohocken, PA, 2017.
- [63] S. Pessiki and A. Pieroni, "Axial load behavior of large-scale spirally-reinforced high-strength concrete columns", *ACI Struct. J.*, vol. 94, no. 3, pp. 304-314, 1997.
- [64] A. Z. Fam and S. H. Rizkalla, "Confinement model for axially loaded concrete confined by circular fiber-reinforced polymer tubes", *ACI Struct. J.*, vol. 98, no. 4, pp. 451-461, 2001.
- [65] *Concrete Structures*, AS 3600:2009, Australian Standard, Sydney, NSW, Australia, 2009.
- [66] J. B. Mander, M. J. Priestley, and R. Park, "Theoretical stress-strain model for confined concrete", *J. Struct. Eng.*, vol. 114, no. 8, pp. 1804-1826, 1988, doi: 10.1061/(ASCE)0733-9445(1988)114:8(1804).